Electronic Supplementary Material (ESI) for RSC Advances.

Supplementary Information for

Rapid Separation and Purification of Lead Halide Perovskite Quantum Dots through Centrifugation in Nonpolar Solvent

Shu Zhou[†,‡,*]

[†] *School of Materials, Sun Yat-sen University, Guangzhou 510275, China*

[‡] *Department of Physics, The Chinese University of Hong Kong, New Territories, Hong Kong*

E-mail: **zhoush67@mail.sysu.edu.cn*

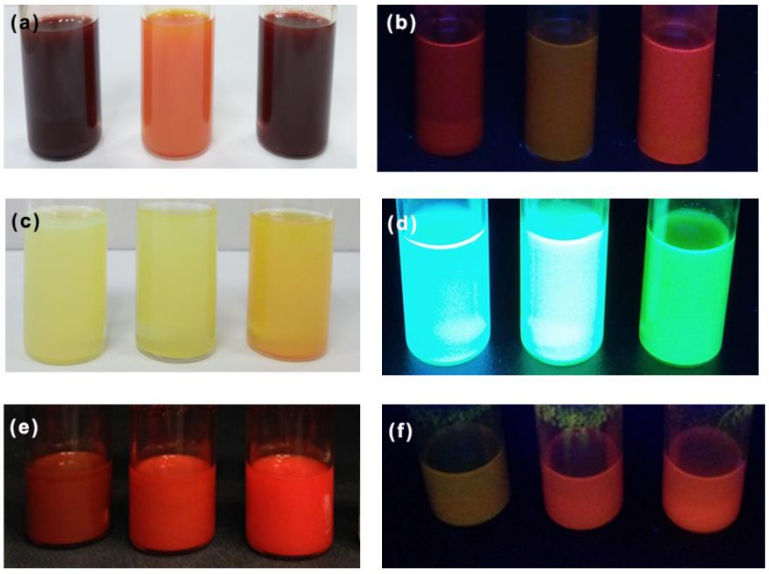

Figure S1. Crude solutions (from left to right, toluene, hexane, chlorobenzene) of (a,b) $MAPbI_3$, (c,d) $MAPbBr_3$ and (e,f) $FAPbI_3$ perovskite quantum dots (QDs) under ambient light and UV light.

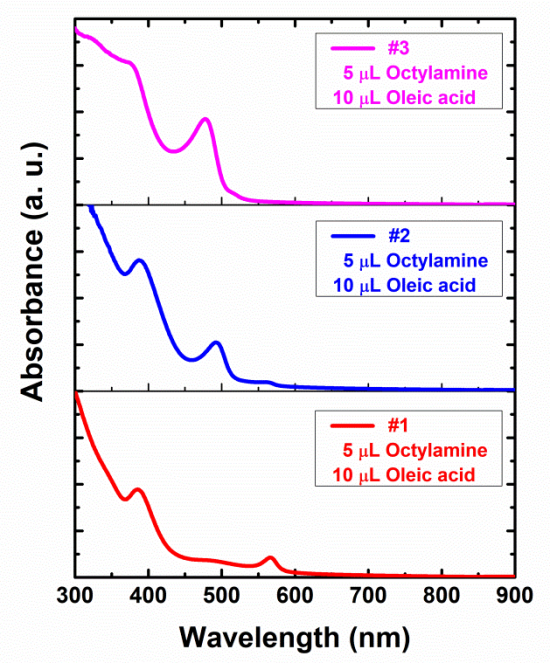

Figure S2. Absorption spectra of crude solutions of $FAPbI_3$ perovskite QDs.

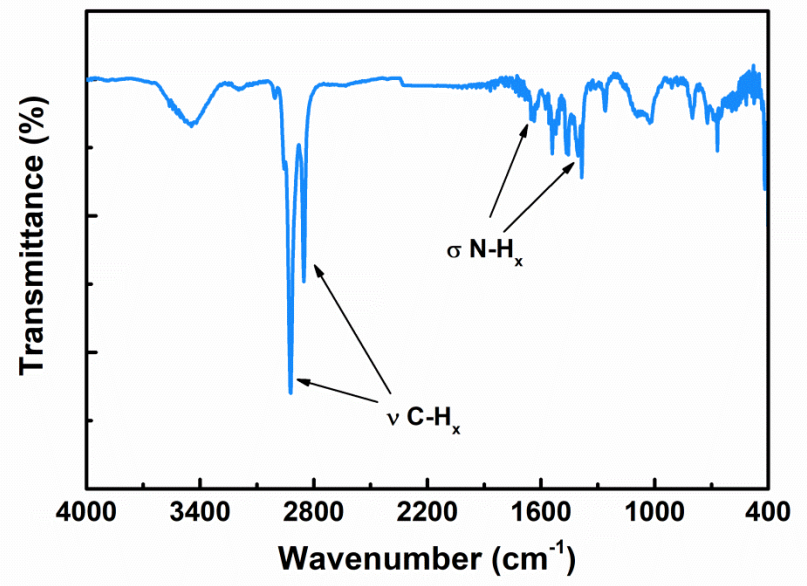

Figure S3. FTIR spectrum of halide perovskite QDs showing extensive alky termination of the QD surface.

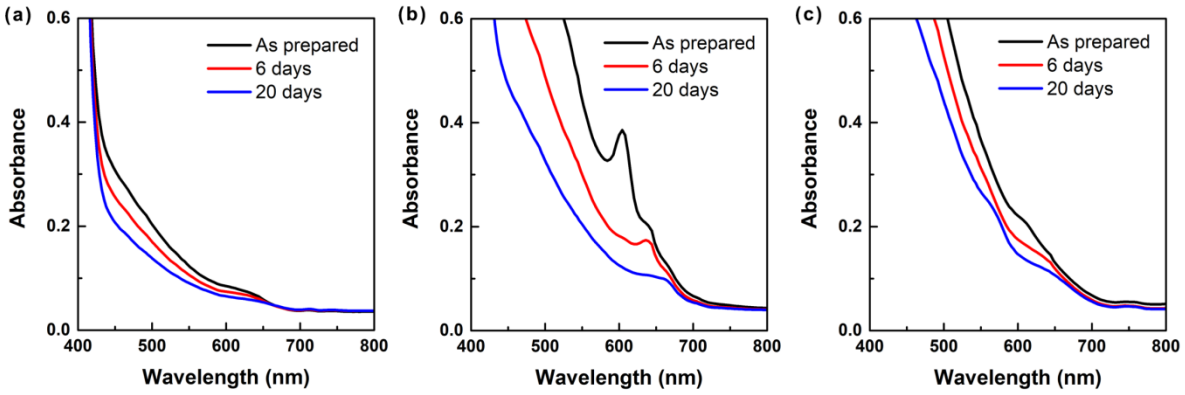

Figure S4. UV-vis absorption of (a) toluene, (b) chlorobenzene and (c) hexane solutions of $MAPbI_3$ perovskite QDs and the same solutions after stored in air for 6 days and 20 days, respectively.

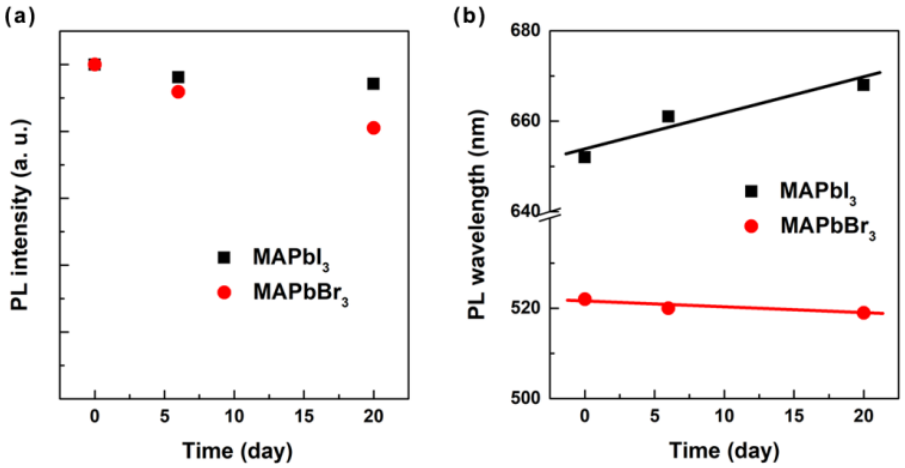

Figure S5. (a) Intensity profile and (b) shift of the PL peak for hexane solutions of $MAPbI_3$ and $MAPbBr_3$ QDs.

As the storage time increases it can be seen that the PL intensity drops by 6% for $MAPbI_3$ hexane solution which is smaller than that of $MAPbBr_3$ hexane solution (19%). By contrast, the PL wavelength of $MAPbI_3$ hexane solution shifts from 652 nm to 668 nm, which is much larger than that of $MAPbBr_3$ hexane solution (from 522 nm to 519 nm). Thus, it may be not accurate to state that the stability of $MAPbI_3$ hexane solution is better than that of $MAPbBr_3$ hexane solution.

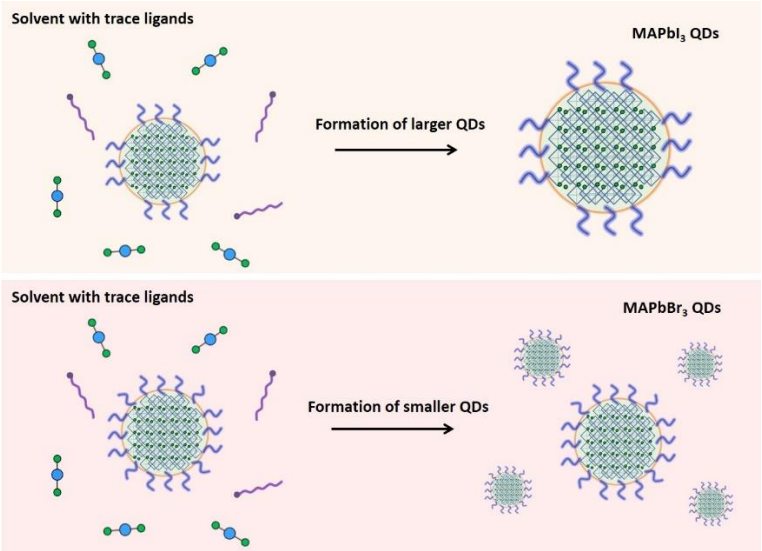

Figure S6. Schematic showing the different transformation processes of $MAPbI_3$ and $MAPbBr_3$ QDs in the solvents during the course of storage in air.

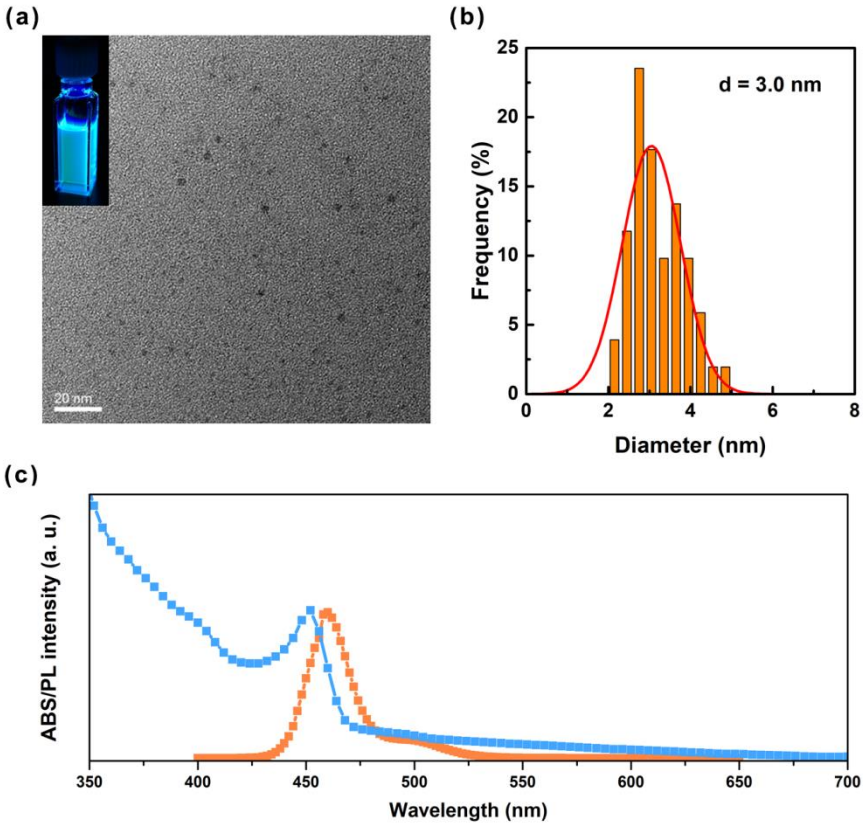

Figure S7. (a-b) TEM image and the corresponding size analysis of monodisperse $CsPbBr_3$ perovskite QDs obtained by differenial centrifugation. (c) UV-vis absorption and PL spectra of $CsPbBr_3$ QD solution after storing in air for 6 days.

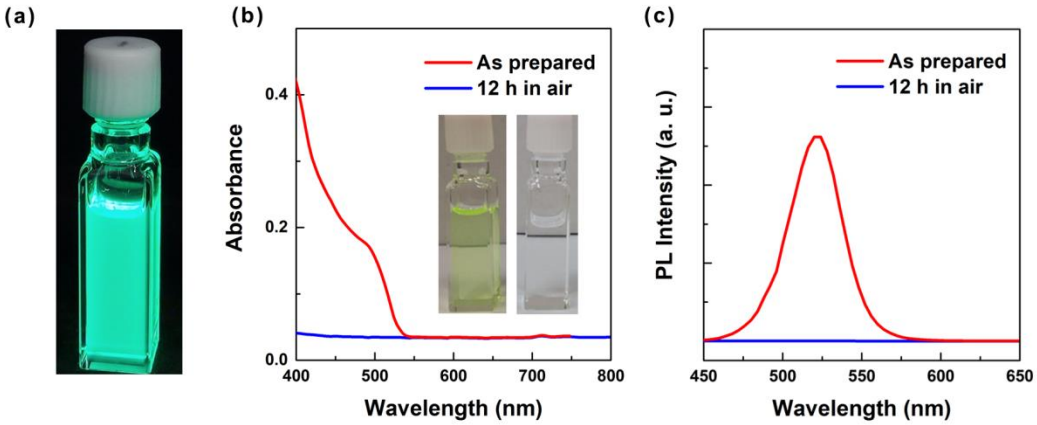

Figure S8. (a) Image of hexane solution of $FAPbBr_3$ perovskite QDs under UV light. (b) UV-vis absorption and (c) PL spectra of $FAPbBr_3$ perovskite QDs solution and the same solution after 12 h storage in air. Inset shows images of hexane solution of $FAPbBr_3$ perovskite QDs and the same solution after 12 h storage in air.

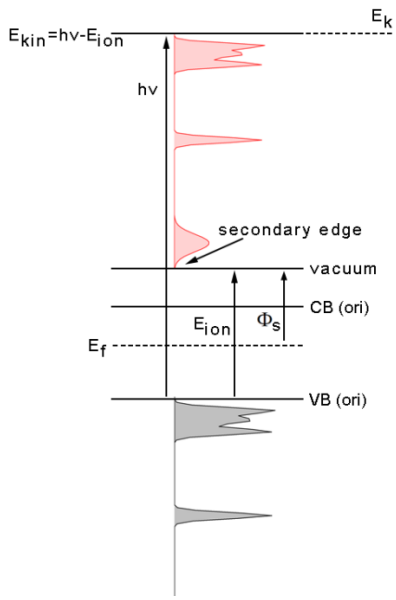

Figure S9. Schematic of photoemission spectroscopy of the perovskite QD samples. Free electrons with certain kinetic energy (E_{kin}) generated by external photoelectric effect depends on the exciting photon energy ($h\upsilon$), the ionization energy (E_{ion}) (or the work function (Φ_s)) of the sample, the binding energy (E_b) of the excited electron, and inelastic scattering processes in the sample.

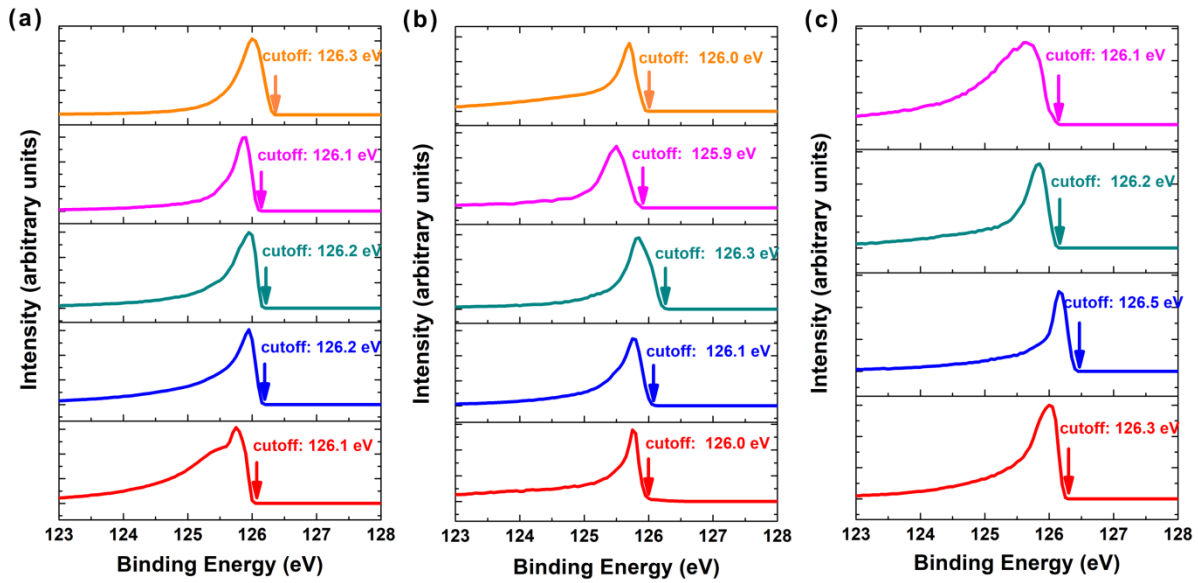

Figure S10. UPS spectra of $MAPbI_3$, $MAPbBr_3$ and $CsPbBr_3$ perovskite QDs with different sizes. The location of Fermi level can be obtained from the secondary cutoff spectra.

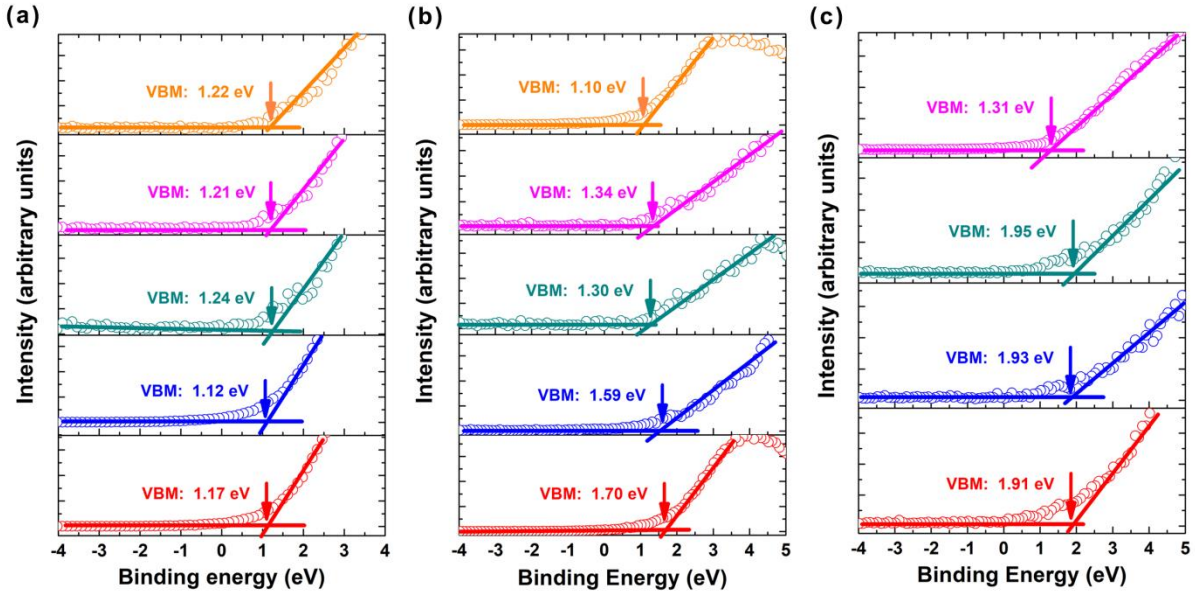

Figure S11. UPS spectra of (a) $MAPbI_3$, (b) $MAPbBr_3$ and (c) $CsPbBr_3$ perovskite QDs with different sizes. The location of HOMO level can be determined from the valence-band maximum (VBM) of the valence band spectra.